Journal of Sound and Vibration (2001) **243**(4), 577–589
doi:10.1006/jsvi.1999.3472, available online at http://www.idealibrary.com on IDEAL®

SYSTEM IDENTIFICATION BASED ON THE DISTRIBUTION OF TIME BETWEEN ZERO CROSSINGS

H. W. SHENTON III AND L. ZHANG

Department of Civil and Environmental Engineering, University of Delaware, Newark, DE 19716, *U.S.A.*

(*Received* 2 *November* 1998, *and in final form* 4 *February* 1999)

A new method for system identification is proposed that is based on fitting the theoretical probability density function (PDF) for the time between zero crossings to a measured distribution of the crossing interval times. Using the theory first developed by Rice, an approximate closed-form expression for the probability density of the time between zero crossings of a linear single-degree-of-freedom system subject to a white noise excitation is obtained. The PDF is a function of the natural frequency and damping ratio of the system, and is accurate for a lightly damped system for time intervals up to the natural period of the system. To estimate the system natural frequency and damping ratio, the PDF is fitted to a histogram of measured crossing interval times, using the Levenberg–Marquardt non-linear least-squares technique. The approach is demonstrated using simulated data for systems with natural frequencies of 0·5, 1·0 and 2·0 Hz and damping ratios of 1, 2·5, 5 and 10%. The method is found to provide good results for the full range of system parameters studied, with errors in the predicted frequency of less than 1·5% and errors in the predicted damping ratio, on an average, less than 7%. The new method is intended to take advantage of technology that now exists in advanced low cost, battery operated, stand-alone instrumentation systems, and will be particularly beneficial in studies of large civil structures.

1. INTRODUCTION

Researchers and engineers are continually working to add to the database of measured natural frequencies, damping ratios and mode shapes of tall buildings, long span bridges and other flexible structures. To do this, any number of traditional methods of system identification may be used with ambient or forced vibration acceleration measurements of the structure under consideration. Some of the classical methods include least squares, maximum likelihood and extended Kalman filter, all of which are based on the analysis of a continuous time history of data. An excellent review of these classical techniques, as they relate to structural engineering, was presented by Imai *et al.* [1]. The data gathered from full scale ambient vibration surveys (AVS) of large structures can be used to verify analytical models, calibrate numerical procedures, design similar structures, and detect structural damage [2].

While they can be extremely useful, ambient vibration surveys of large civil structures are only rarely conducted. One reason for this is the high cost and labor associated with a comprehensive test, which is directly correlated to the size of the test "specimen". Full-scale civil "specimens" (i.e., building, bridge or tower) are generally of the order of hundreds or thousands of meters in length or width. Using traditional sensors and recording devices the set-up time needed to record just a few minutes of data can take days or even weeks. Size also has an impact on the number of transducers that can be deployed,

0022-460X/01/240577 + 13 $35.00/0

the number of different test configurations that one can use, the amount of data that is collected, and ultimately the quality of the identified properties of the system. As a result, vibration surveys of large civil structures are not routinely conducted.

Recent advances in sensor and microprocessor technology may soon change this situation. Advanced instrumentation systems have recently been developed that record, process and store data in local memory. These "intelligent" instruments are small, have on-board microprocessors and storage media, can be battery operated, and are intended to operate in a stand-alone mode free of cabling and an external recording device. There are instruments that can record and store a continuous time history of measured data, much like a traditional sensor and recording system. They have the advantage that they do not require cables and an external data acquisition system, and the data collected is amenable to traditional methods of system identification.

Another very unique instrumentation system, referred to here as an "acceleration peak meter", records and stores only the peak acceleration of a shock event. The impetus for development of this instrument was to monitor cargo as it is shipped around the world. In this application, the peak meter is mounted on a shipping container at the point of departure, and configured to trigger whenever the cargo experiences a shock above a specified threshold. While in route, the system waits for a trigger due to some type of shock loading. Once triggered, it records and stores only four data values from the event: peak acceleration, time at which the trigger threshold was exceeded, change in velocity and the duration of the event (time between the up- and down-crossing of the threshold). The actual time history of the event is discarded. The instrument then re-arms itself and waits for the next trigger. By doing this it compiles a history of the shocks experienced by the cargo during its journey, storing only the most important information. Once the cargo reaches its final destination the data stored in the instrument is down loaded and interrogated and used to help explain any damage that might be observed in the cargo. The device is compact, battery operated, and relatively inexpensive. Although originally developed for monitoring cargo, the peak meter technology may be exploited for system identification of large civil structures, with perhaps significant benefits.

These new instruments, and other wireless technologies, have great potential for use in vibration monitoring of large civil structures. However, in order to take advantage of some of them, new methods for system identification need to be developed that are tailored to the capabilities of the system. To take advantage of the amplitude and threshold crossing interval data provided by the acceleration peak meter, a new method for system identification has been developed that is based on fitting the theoretical probability density function (PDF) for the time between zero crossings to the measured distribution of the crossing interval times.

Presented in the paper are the results of a study, the objective of which was to develop a method for system identification that is based on the distribution of time between zero crossings. In the following, a brief overview of the proposed methodology, the theory, a description of the numerical simulations used to test the methodology, followed by the results and discussion are presented.

2. METHODOLOGY

The method proposed is based on having only a record or ensemble of the zero crossing times from ambient vibration measurements of a structure. For now, scope is limited to determining the natural frequency and damping ratio of a linear single-degree-of-freedom (s.d.o.f.) system, subject to a white noise excitation (a common assumption in AVS of large civil structures). Future work will extend the method to include multi-degree-of-freedom systems and the determination of mode shapes.

Consider a linear s.d.o.f. system, for which the governing equation of motion is

$$\ddot{x} + 2\zeta\omega_n\dot{x} + \omega_n^2 x = f(t)/m, \tag{1}$$

in which ω_n is the natural frequency, ζ the damping ratio, m the mass, and x, $\dot{x}$ and $\ddot{x}$ denote the displacement, velocity and acceleration of the system respectively. The force $f(t)$ is assumed to be a stationary white noise excitation with constant power spectral density, S_0.

The response of the linear system is a stationary random process; an example of the response is shown in Figure 1. For a lightly damped structure, the time history resembles simple harmonic motion, with an average frequency equal to ω_n and a randomly varying amplitude.

From the measured time history the zero crossing times are identified, as shown in Figure 1. From these, the time between successive zero crossings is calculated, i.e., $\Delta T_i = T_{i+1} - T_i$. Note that ΔT is a random variable; for a lightly damped system, ΔT should be approximately equal to $T_n/2 = \pi/\omega_n$. The mean and variance of ΔT_i, however, will vary depending on the damping in the system.

Using the ΔT_i collected from a sample record, a histogram of the time between zero crossings is constructed. The histogram is indicative of the probability density function of the time between crossings, and presumably would be a function of the natural frequency and damping ratio of the system. Provided the theoretical PDF can be determined in closed form, and in terms of the system properties, then ω_n and ζ can be determined by fitting the theoretical distribution to measured distributions. This is the basis for the system identification technique. In the next section, the theoretical PDF for the time between zero crossings is derived.

2.1. THEORETICAL PDF OF TIME BETWEEN ZERO CROSSINGS

Researchers have been interested in the statistics of stochastic processes for many years. A tremendous amount of work has been focused on understanding the statistics of threshold crossings and the distribution of extrema magnitude. A much more complex

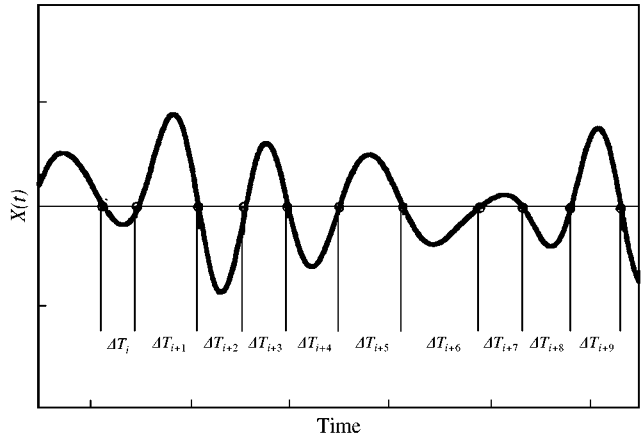

Figure 1. Sample response and identification of the zero crossing intervals for a single-degree-of-freedom system subject to white noise.

problem deals with the statistics of the time between threshold crossings and the time between extrema. Blake and Lindsey [3] provide an excellent review of research on the level crossing problem.

In 1945, Rice [4] derived an approximate expression for the PDF of the zero crossings intervals of a random noise current, I. Rice's work, summarized below, is used as the basis for deriving an approximate expression for the PDF of time between zero crossings used in the system identification procedure.

Rice derived the following expression for the probability of noise current, I, passing through zero in the interval τ, $\tau + \mathrm{d}\tau$ with a negative slope, when it is known that I passes through zero at $\tau = 0$ with a positive slope:

$$P(\tau) = (\mathrm{d}\tau/2\pi)[\psi_0/-\psi''_0]^{1/2}[M_{23}/H](\psi_0^2 - \psi_\tau^2)^{-3/2}[1 + H\cot^{-1}(-H)], \tag{2}$$

in which

$$H = M_{23}[M_{22}^2 - M_{23}^2]^{-1/2}, \tag{3}$$

and M_{22} and M_{23} are the cofactors of $\mu_{22} = -\psi''_0$ and $\mu_{23} = -\psi''_\tau$ in the matrix

$$\mu = \begin{bmatrix} \psi & 0 & \psi'_\tau & \psi\tau \\ 0 & -\psi''_0 & -\psi''_\tau & -\psi'_\tau \\ \psi'_\tau & -\psi''_\tau & -\psi''_0 & 0 \\ \psi_\tau & -\psi'_\tau & 0 & \psi_0 \end{bmatrix}. \tag{4}$$

In the matrix above, $\psi_\tau = \psi(\tau)$ is the autocorrelation function for the noise current I, $(\cdot)'$ denotes differentiation with respect to τ, and a subscript 0 denotes evaluation at $\tau = 0$. Evaluating the cofactors yields

$$M_{22} = -\psi''_0(\psi_0^2 - \psi_\tau^2) - \psi_0(\psi'_\tau)^2, \qquad M_{23} = \psi''_\tau(\psi_0^2 - \psi_\tau^2) + \psi_\tau(\psi'_\tau)^2. \tag{5, 6}$$

In these expressions, Rice chose $0 \leqslant \cot^{-1}(-H) \leqslant \pi$, the value π being taken at $\tau = 0$ and $\pi/2$ as $\tau \to \infty$. Following the general derivation, Rice derived an approximate closed-form expression for the PDF of zero crossings for an ideal band pass filter.

The objective here is to determine the probability density function of the time between zero crossings of displacement of the linear s.d.o.f. system. This can be derived from equation (2) when the autocorrelation function in equation (4) corresponds to the autocorrelation for displacement of the s.d.o.f. system.

The power spectral density of displacement of the s.d.o.f. system subject to a white noise excitation with spectral amplitude S_0 is

$$S_x(f) = |H(f)|^2 S_0 = S_0 f_n^4/k^2|f^4 + (4\zeta^2 - 2)f_n^2 f^2 + f_n^4|, \tag{7}$$

in which $H(f)$ is the complex frequency response function for the system and f_n is the natural frequency in Hz. The autocorrelation function for displacement is determined from equation (7) using the Wiener–Khinchine relation, i.e.,

$$\psi_x(\tau) = \int_0^\infty S_x(f)\cos(2\pi\tau f)\,\mathrm{d}f. \tag{8}$$

Substituting equation (7) into equation (8) and evaluating yields

$$\psi_x(\tau) = \left(\frac{S_0}{k^2}\right)\left(\frac{\pi}{4}f_n\right)\mathrm{e}^{-2\pi\tau f_n\zeta}\left[\frac{\cos(2\pi\tau f_n\sqrt{1-\zeta^2})}{\zeta} + \frac{\sin(2\pi\tau f_n\sqrt{1-\zeta^2})}{\sqrt{1-\zeta^2}}\right]$$

$$= (S_0/k^2)F_1(f_n,\zeta). \tag{9}$$

The function $F_1(f_n,\zeta)$ and similar functions that follow has been introduced to represent the expression to the right of equation (9) that is only a function of the natural frequency f_n and the damping ratio ζ.

The first and second derivatives of $\psi_x(\tau)$ with respect to τ are

$$\psi'_x(\tau) = -\left(\frac{S_0}{k^2}\right)\frac{\pi^2 f_n^2}{2\zeta\sqrt{1-\zeta^2}}\,\mathrm{e}^{-2\pi\tau f_n\zeta}\sin(2\pi\tau f_n\sqrt{1-\zeta^2})$$

$$= (S_0/k^2)F_2(f_n,\zeta), \tag{10}$$

$$\psi''_x(\tau) = \left(\frac{S_0}{k^2}\right)(\pi^3 f_n^3)\,\mathrm{e}^{-2\pi\tau f_n\zeta}$$

$$\times\left[\frac{\sin(2\pi\tau f_n\sqrt{1-\zeta^2})}{\sqrt{1-\zeta^2}} - \frac{\cos(2\pi\tau f_n\sqrt{1-\zeta^2})}{\zeta}\right]$$

$$= (S_0/k^2)F_3(f_n,\zeta). \tag{11}$$

Evaluating equations (9)–(11) at $\tau = 0$ yields

$$\psi_x(0) = \left(\frac{S_0}{k^2}\right)\frac{\pi f_n}{4\zeta} = \left(\frac{S_0}{k^2}\right)F_4(f_n,\zeta), \quad \psi'_x(0) = 0, \tag{12, 13}$$

$$\psi''_x(0) = -\left(\frac{S_0}{k^2}\right)\times\frac{\pi^3 f_n^3}{\zeta} = \left(\frac{S_0}{k^2}\right)F_5(f_n,\zeta). \tag{14}$$

Substituting equations (9)–(14) into the equations for M_{22} and M_{23} yields

$$M_{22} = (S_0/k^2)^3 F_6(f_n,\zeta), \qquad M_{23} = (S_0/k^2)^3 F_7(f_n,\zeta) \tag{15, 16}$$

in which

$$F_6 = -F_5(F_4^2 - F_1^2) - F_4 F_2^2, \qquad F_7 = F_3(F_4^2 - F_1^2) + F_1 F_2^2. \tag{17, 18}$$

Substituting equations (17) and (18) in the expression for H and simplifying yields

$$H = F_7[F_6^2 - F_7^2]^{-1/2} = F_8(f_n,\zeta). \tag{19}$$

Finally, substituting equations (9), (12), (14), (16) and (19) into equation (2) and simplifying yields

$$P(\tau) = \frac{d\tau}{2\pi}\left[\frac{F_4}{-F_5}\right]^{1/2}\left[\frac{F_7}{F_8}\right][(F_4^2 - F_1^2)]^{-3/2}[1 + F_8\cot^{-1}(-F_8)]$$

$$= \frac{d\tau}{2\pi}\left[\frac{F_4}{-F_5}\right]^{1/2}\frac{(F_6^2 - F_7^2)^{1/2}}{(F_4^2 - F_1^2)^{3/2}}[1 + F_8\cot^{-1}(-F_8)]. \quad (20)$$

Equation (20) is an approximation of the probability density function of the time between zero crossings of displacement of a linear s.d.o.f. system subject to a stationary white noise input. Details are not presented but it can be shown that the coefficients (S_o/k^2) completely cancel in equation (20), i.e., the function is independent of the spectral amplitude of the white noise input, as would be expected for a linear system; therefore, equation (20) is only a function of f_n and ζ.

Equation (20) is plotted in Figure 2 for $f_n = 1{\cdot}5$ Hz and $\zeta = 3\%$, versus τ/T_n. Note that the density function has peaks near $\tau = 0{\cdot}333 = 0{\cdot}5T_n$, $1{\cdot}0 = 1{\cdot}5T_n$, $1{\cdot}666 = 2{\cdot}5T_n$, and $2{\cdot}333 = 3{\cdot}5T_n$ s, and multiples thereof, in which T_n is the fundamental period of the system. The approximation becomes invalid for large τ, as noted by the finite asymptote at large τ. The density function exceeds the probability that x will cross-zero at $\tau = 0$ and in τ, $\tau + d\tau$, without any other zero crossings in between, since it includes all of the latter, plus any that have an even number of crossings between 0 and τ, $\tau + d\tau$ [4]. For a lightly damped s.d.o.f. system, however, it is unlikely that an even number of multiple crossings will take place between $\tau = 0$ and $\tau = T_n/2$ (or for that matter, any number of multiple crossings). McFadden [5] generalized the work of Rice to that of non-Gaussian noise and in doing so argued that for a narrow band spectrum, Rice's equation is a close approximation up to $1{\cdot}5T_n$, i.e., the practical range of τ. Therefore, one can assume that equation (20) is a reasonable approximation to the PDF of time between zero crossings, out to a τ of approximately T_n. For the identification technique, equation (20) is used only out to about $\tau = T_n$.

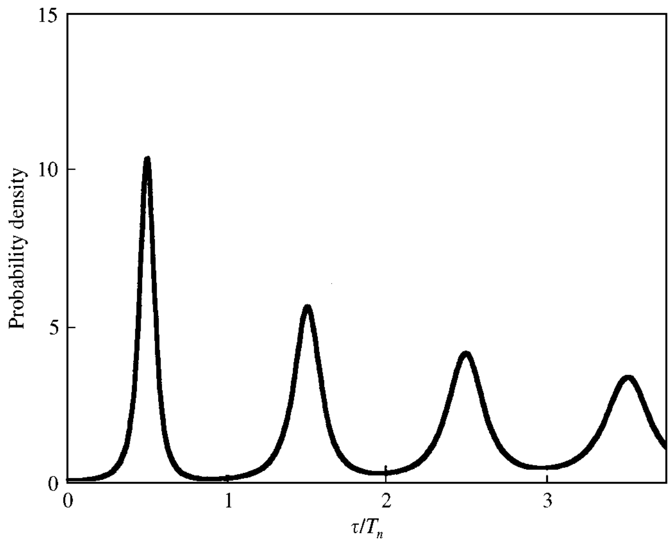

Figure 2. Theoretical probability density function for the time between zero crossings [equation (20)].

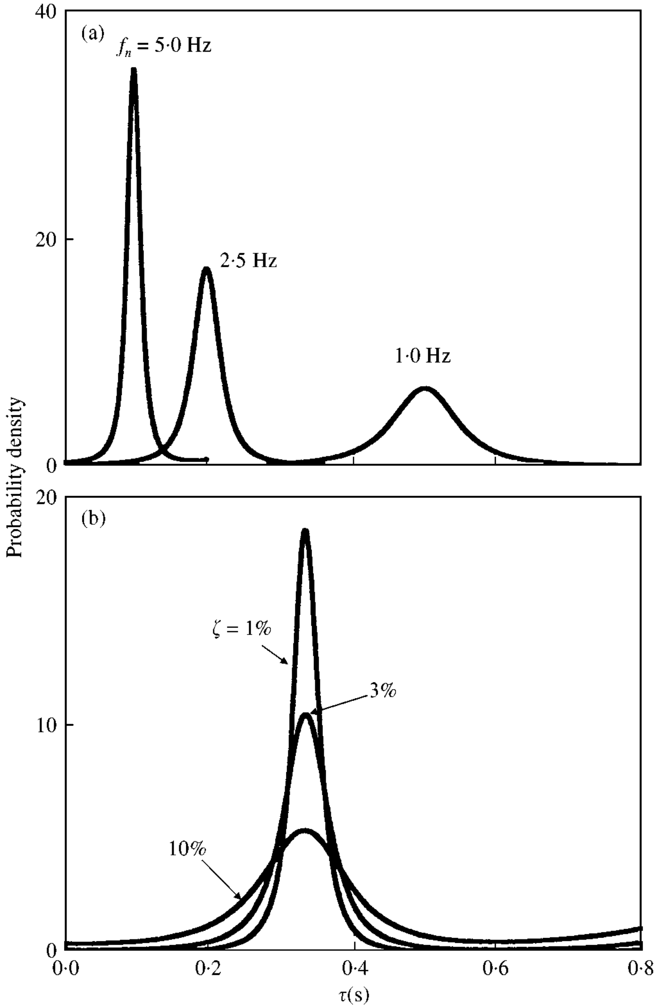

Figure 3. Probability density function for varying natural frequency and damping ratios: (a) $\zeta = 3\%$; (b) $f_n = 1{\cdot}5$ Hz.

Equation (20) is plotted in Figure 3 for a range of frequencies and damping ratios. Presented in Figure 3(a) is a plot of the PDF for various f_n and a damping ratio of $\zeta = 3\%$; presented in Figure 3(b) is the PDF for fixed $f_n = 1{\cdot}5$ Hz and damping ratios of $\zeta = 1$, 3 and 10%. Note that the PDF closely resembles a normal distribution, particularly for lightly damped systems. For a lightly damped system, the distribution is very narrow and is concentrated around the mean of approximately $T_n/2$. The distribution becomes much broader as the damping ratio is increased and the peak is not well defined. There is also a very small decrease in the mean value with increasing ζ.

The trends noted in the probability density function in Figure 3 that occur with changes in frequency and damping ratio can be explained by considering the power spectrum of the system response for varying parameters. Consider first the result shown in Figure 3(a); for fixed ζ, the peak in the PDF shifts to $\tau \approx T_n/2$ and becomes sharper with increasing f_n. The shift to $\tau \approx T_n/2$ is obvious since the predominant frequency of the response is the natural frequency in each case. Recall, however, that the half-power bandwidth of the response of a linear, viscously damped, s.d.o.f. system is approximately equal to $2\zeta\omega_n = 4\pi\zeta f_n$, and the resonant amplitude of the spectrum does not change with frequency. This implies that the energy of the system response at $f \approx f_n$, increases with increasing f_n. Therefore, the system with the higher natural frequency has more energy at the natural frequency, which tends to increase the likelihood that the next zero crossing will be closer to $T_n/2$. This in turn results in a sharper PDF. Finally, consider the results shown in Figure 3(b); for fixed f_n, the PDF decreases and becomes less sharp with increasing damping. In this case, while the half-power bandwidth does increase with increasing damping, the amplitude of the response decreases. This decreases the energy of the system response at $f \approx f_n$ and results in a more broadbanded response. Therefore, the likelihood of the next zero crossing occurring at $T_n/2$ decreases and the resulting PDF decreases.

The theoretical PDF of the time between zero crossings is strongly dependent on the dynamic characteristics of the system. The procedure for identifying the dynamic characteristics of the system is based on fitting the measured distribution to the theoretical density function in equation (20). The approach is illustrated in the next section using simulated data.

3. NUMERICAL SIMULATIONS

To test the proposed method for system identification, simulated response time histories were generated for an s.d.o.f. system subject to a stationary white noise excitation. The theoretical probability density function presented in equation (20) was then fitted to the simulated ΔT distributions to yield the estimated natural frequency and damping ratio of the system. Details of the procedure are described below.

Response time histories were generated by solving equation (1) using MATLAB, for a random white noise excitation. Time histories were generated for a total of 12 s.d.o.f. systems, with natural frequencies equal to 0·5, 1·0 and 2·0 Hz, and damping ratios of 1, 2·5, 5 and 10%.

The force excitation was generated from a sum of harmonics with random phase angles, i.e., using the relation

$$f(t) = \sin(\omega_0 t + \phi_0) + \sum_{i=1}^{n} \sin(\mathrm{i}\Delta\omega t + \phi_i). \tag{21}$$

In the previous equation, ω_0 is the starting frequency, $\Delta\omega$ is the frequency resolution and ϕ_i is a random phase angle in the range $0-2\pi$ that occurs with uniform probability. In that it is not possible to generate a true white excitation, a band-limited force was created with frequencies ranging from 0·01 to 19·99 Hz [$\omega_0 = 0{\cdot}0628$ rad/s (0·01 Hz), $\Delta\omega = 0{\cdot}125$ rad/s (0·02 Hz) and $n = 999$ in equation (21)]. Note that the natural frequencies of the s.d.o.f. systems considered were all well within the frequency band of the force excitation. A total of 24 unique force time histories were generated, each with a duration of 60 s and a time increment of 0·01 s: multiple force time histories were used to facilitate the post-processing of the data. All of the force time histories were scaled to have an r.m.s. value of 1.

From the computed time histories of response, the zero crossings were identified and the ΔT_i between crossings determined. In extracting the crossing information, the first 10 s of each record was ignored so that the distributions would not be affected by the transient response of the system. A minimum of 1200 zero crossings intervals were compiled for each system. The ΔT's collected from the different time histories, corresponding to the different

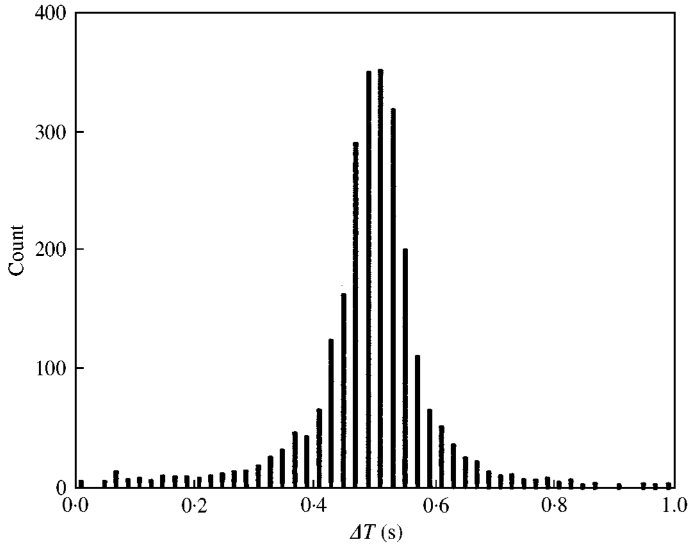

Figure 4. Sample histogram of zero crossing intervals for $f_n = 1$ Hz and $\zeta = 2{\cdot}5\%$.

forces time histories, were combined into one data set, as though they were obtained from a single, long response time history. A sample histogram for $f_n = 1$ Hz and $\zeta = 2{\cdot}5\%$ is shown in Figure 4.

Histograms of the crossing intervals were created and normalized such that the total count was one (i.e., the area under the histogram was one). Equation (20) was then fitted to the histogram of simulated data using the Levenberg–Marquardt non-linear least-squares approach [6], to yield the estimate of the natural frequency and damping ratio of the system. The fitting was conducted using a commercial data analysis and plotting program, running on a desktop personal computer. Initial estimates of the unknown frequency and damping ratio were needed to start the process; the sensitivity of the method to these initial guesses is discussed later.

4. RESULTS AND DISCUSSION

Presented in Figures 5–7 are the results for the systems with natural frequencies of 0·5, 1·0 and 2·0 Hz respectively. Presented to each figure are the results for the four different damping ratios: 1, 2·5, 5 and 10%. The simulated distributions are shown by the underlying histogram; the results of fitting equation (20) to the simulated distribution is shown by the solid curve. The estimated properties are indicated in the figure caption by f_{fit} and ζ_{fit}. The results of the system identification are summarized in Table 1, in which are presented the actual properties, the estimated properties, the error in the predicted frequency and damping ratio, and the correlation coefficient (R).

In general, there is a very good agreement between the true properties and the predicted natural frequency and damping ratio. The fits are very good for all values of f_n and ζ as indicated by the correlation coefficient in the table. The results are slightly better, however, for higher values of the natural frequency and lower values of damping. One reason for this is the number of crossing intervals in the histogram. With the 24 time histories, the number

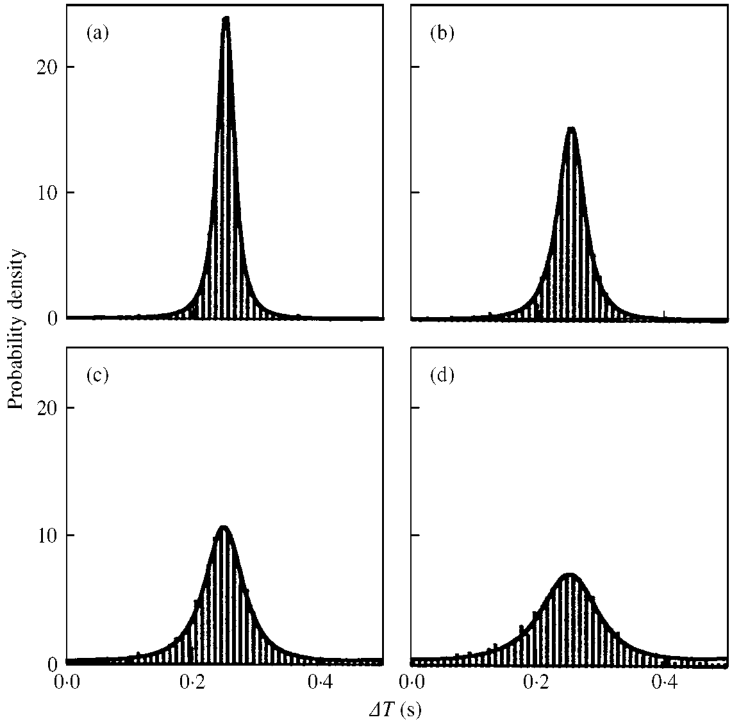

Figure 5. Histograms of zero crossing intervals and fitted PDF for $f_n = 2{\cdot}0$ Hz and varying damping ratios: (a) $\zeta = 1\%$, $f_{fit} = 1{\cdot}998$ Hz, $\zeta_{fit} = 1{\cdot}02\%$; (b) $\zeta = 2{\cdot}5\%$, $f_{fit} = 1{\cdot}999$ Hz, $\zeta_{fit} = 2{\cdot}47\%$; (c) $\zeta = 5\%$, $f_{fit} = 2{\cdot}002$ Hz, $\zeta_{fit} = 4{\cdot}90\%$ and (d) $\zeta = 10\%$, $f_{fit} = 1{\cdot}995$ Hz, $\zeta_{fit} = 9{\cdot}93\%$.

of crossing intervals obtained from the simulations was higher for the higher natural frequencies: ~ 4800 for $f_n = 2$ Hz, versus ~ 2400 for $f_n = 1{\cdot}0$ Hz, versus ~ 1200 for $f_n = 0{\cdot}5$ Hz. Thus, because of the larger sample size, the histograms for the higher natural frequency are somewhat smoother and therefore lead to better fits. Similarly, for the same f_n, the larger the variance of the time intervals, the greater the damping ratio. Therefore, with the same bin size and approximately the same number of crossing intervals, the histogram for the lower damping ratio is smoother than the one for the higher damping ratio and therefore leads to a better fit.

In performing the curve fits, initial estimates of the system properties are needed to start the process. Once the histogram is constructed, an initial guess for the natural frequency becomes evident from the peak in the histogram near $0{\cdot}5T_n$. At that point, the data can be re-binned to a convenient resolution, which for the results shown in Figures 5–7 was taken to be $T_n/50$, and then normalized such that the area under the histogram is one. An initial value for the damping ratio must then be selected. For a typical civil structure, this would be in the range of 1–5%. Tests were conducted to examine the sensitivity of the results to the initial estimates. For these informal tests, the initial guess for the frequency was varied from the true values by $\pm 20\%$ and the initial guess for the damping ratio was varied by more than 100%. Results show that the fit procedure is more sensitive to the initial estimate of the natural frequency than the initial estimate of the damping ratio. Results converged to the true values for initial frequencies within 10% of the true value, and the damping ratios that differed from the true value by more than 100%. In a practical application, the sensitivity to

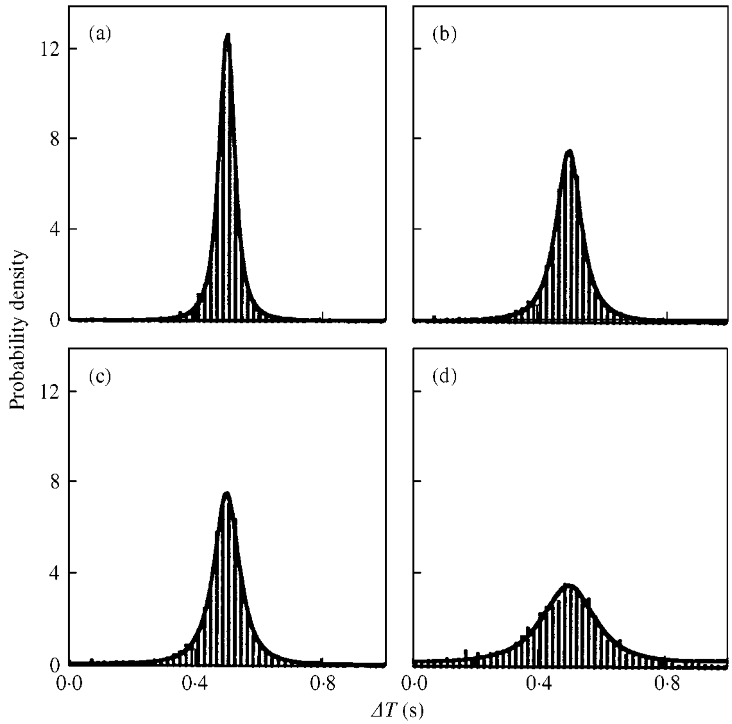

Figure 6. Histograms of zero crossing intervals and fitted PDF for $f_n = 1{\cdot}0$ Hz and varying damping ratios: (a) $\zeta = 1\%$, $f_{fit} = 0{\cdot}997$ Hz, $\zeta_{fit} = 0{\cdot}93\%$; (b) $\zeta = 2{\cdot}5\%$, $f_{fit} = 0{\cdot}995$ Hz, $\zeta_{fit} = 2{\cdot}48\%$; (c) $\zeta = 5\%$, $f_{fit} = 0{\cdot}998$ Hz, $\zeta_{fit} = 5{\cdot}24\%$ and (d) $\zeta = 10\%$, $f_{fit} = 0{\cdot}986$ Hz, $\zeta_{fit} = 9{\cdot}70\%$.

the initial frequency should not be a problem since an accurate estimate of f_n can be obtained just from the histogram.

5. CONCLUSIONS

A new method for system identification has been developed that is based on fitting the theoretical probability density function (PDF) for the time between zero crossings to a measured distribution of the crossing interval times. Using the theory first developed by Rice, an approximate closed-form expression for the probability density of the time between zero crossings of a linear s.d.o.f. system subject to a white noise excitation was obtained. The approximate distribution is expected to be accurate for a lightly damped system, up to a crossing interval length equal to the natural period of the system.

The identification procedure is based on having an ensemble of measured interval crossings for a s.d.o.f. system subject to a stationary white noise excitation (a typical assumption for an ambient vibration survey of a large civil structure). The theoretical PDF is then fit to the histogram of measured crossing intervals, using the non-linear least-squares approach of Levenberg–Marquardt to yield the estimate of the natural frequency and damping ratio.

The procedure has been tested using simulated data. Response time histories were generated for a s.d.o.f. system, for a range of frequencies and damping ratios. The system properties were then estimated using the distribution of zero crossing intervals. Results have been shown to be in good agreement, with the maximum error in the predicted frequency of

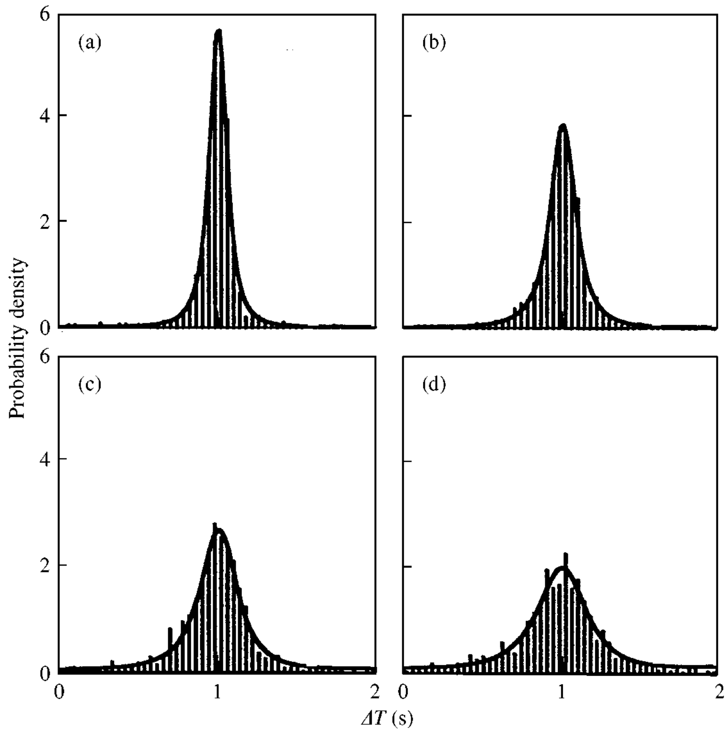

Figure 7. Histograms of zero crossing intervals and fitted PDF for $f_n = 0{\cdot}5$ Hz and varying damping ratios: (a) $\zeta = 1\%$, $f_{fit} = 0{\cdot}499$ Hz, $\zeta_{fit} = 1{\cdot}17\%$; (b) $\zeta = 2{\cdot}5\%$, $f_{fit} = 0{\cdot}498$ Hz, $\zeta_{fit} = 2{\cdot}45\%$; (c) $\zeta = 5\%$, $f_{fit} = 0{\cdot}496$ Hz, $\zeta_{fit} = 4{\cdot}77\%$ and (d) $\zeta = 10\%$, $f_{fit} = 0{\cdot}499$ Hz, $\zeta_{fit} = 8{\cdot}20\%$.

TABLE 1

Frequencies and damping ratios estimated from simulated data

f_n (Hz)	ζ%	f_{fit} (Hz)	%Error	ζ_{fit}%	%Error	R
2·0	1·0	1·998	0·1	1·02	2·0	0·999
2·0	2·5	1·999	0·05	2·47	1·2	0·999
2·0	5·0	2·002	0·1	4·90	2·0	0·997
2·0	10·0	1·995	0·25	9·93	0·7	0·990
1·0	1·0	0·997	0·3	0·93	7·0	0·999
1·0	2·5	0·995	0·5	2·48	0·8	0·997
1·0	5·0	0·998	0·2	5·24	4·8	0·993
1·0	10·0	0·986	1·4	9·70	3·0	0·986
0·5	1·0	0·499	0·2	1·17	17	0·995
0·5	2·5	0·498	0·4	2·45	2	0·995
0·5	5·0	0·496	0·8	4·77	4·6	0·990
0·5	10·0	0·499	0·2	8·20	18	0·977

less than 2%, and the error in the predicted damping ratio, on an average less than 7%. In a few cases, the predicted damping ratios were in error by as much as 19%, but this can be attributed to the number of crossing intervals (i.e., count) and the higher damping ratio.

For now, scope has been limited to determining the natural frequency and damping ratio of a linear s.d.o.f. system. Work is continuing to develop a procedure for estimating the mode shape and also to verify the procedure experimentally. Future work could extend the procedure to include or make use of the distribution of time between local maxima and minima, and the distribution of crossing intervals for threshold values other than zero.

The proposed method for system identification is intended to make use of new advanced sensors and instruments that have been developed in recent years, namely a stand-alone digital peak meter. The methodology, in conjunction with the peak meter, has the potential to greatly reduce time, labor and cost of conducting ambient vibration surveys of large civil structures. This will help in expanding all the important database of measured properties for large civil structures.

ACKNOWLEDGMENTS

The authors would like to thank the University of Delaware Research Foundation for their financial support of the research described herein.

REFERENCES

1. H. Imai, C. B. Yun, O. Maruyama and M. Shinozuka 1989 *Probabilistic Engineering Mechanics* **4**, 162–173. Fundamentals of system identification in structural dynamics.
2. C. R. Farrar, S. W. Doebling, G. H. James and T. Simmermacher 1997 *Proceedings of the International Workshop on Structural Health Monitoring, Stanford University, Stanford, CA*, September 18–20. Structural health monitoring activities at national laboratories.
3. I. F. Blake and W. C. Lindsey 1973 *IEEE Transactions on Information Theory* **19**, 295–315. Level-crossing problems for random processes.
4. S. O. Rice 1945 *Bell Systems Technology Journal* **24**, 46–156. Mathematical analysis of random noise.
5. J. A. McFadden 1956 *IEEE Transactions on Information Theory* **2**, 146–150. The axis crossing intervals of random functions.
6. W. H. Press, S. A. Teukolsky, W. T. Vetterling and B. R. Flannery 1992 *Numerical Recipes in C: The Art of Scientific Computing*. Cambridge: Cambridge University Press.